Supplementary Figure 1. Folding and unfolding pathways of the KC30 RNA.

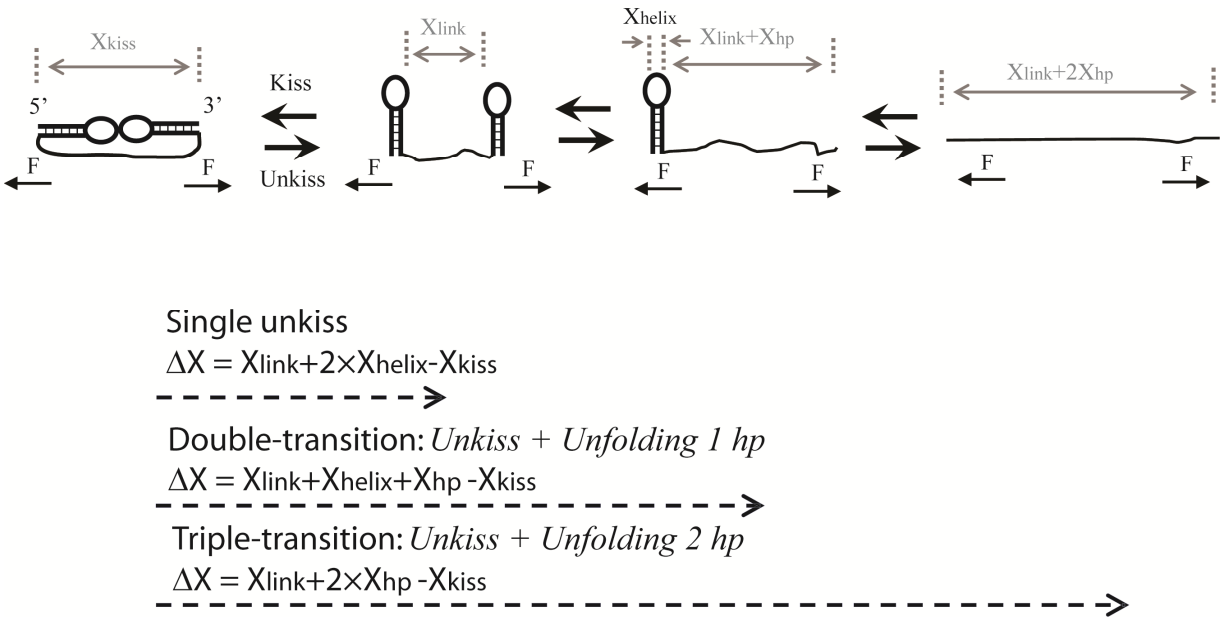

Mechanical unfolding pathways of the KC30 RNA was characterized previously (1). As force is raised, the kissing complex is sequentially unfolded into two linked hairpins, one hairpin, and a single strand. Refolding reverses the unfolding pathway. Because the unkiss occurs at high forces on occasions, the first rip may represent the unkiss alone, double-transition, and triple-transition. $\Delta X_{single\text{-}rip}$ in the KC30 depends on the unfolding pathway (1).

Supplementary Figure 2. Predicted ΔX_{unkiss} in the KC15 and KC30 RNAs.

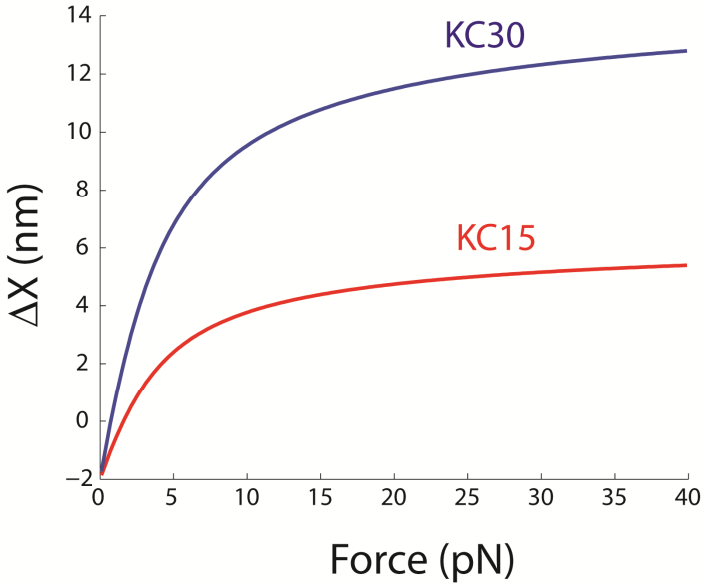

Based on the unfolding model in the Supplementary Fig.1, we computed ΔX_{unkiss} as a function of force. The KC15 shows a small signal in extension change for the unkiss, especially at forces lower than 10 pN.

Supplementary Figure 3. Force dependent unkiss rates of the KC15 and KC30 RNAs.

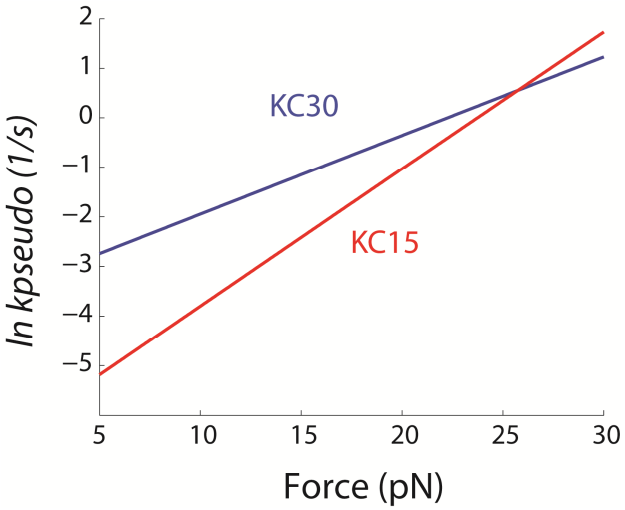

The unkiss rate of the KC30 was extrapolated from unkiss force distribution (Figs 3a-c). Similar calculation on the KC15 was based on the single-rip force distribution (Fig. 3f), assuming the other two types of trajectories had no kissing interaction. The two-step unfolding (Fig. 3e) may involve breaking a kissing complex. Because of its rarity, the four trajectories do not significantly change the analysis. The force distribution was fit to the following equation (2):

$$\ln[r\ln[1/N(F,r)]] = [k_0 - \ln(X^{\ddagger}/\mathrm{k_B T})] + (X^{\ddagger}/k_B T)F$$

in which $N(F,r)$ is the fraction of folded molecule at force F and loading rate r; k_0 is a factor reflecting both the rate constant at zero force and instrumental factors; $X^{\ddagger}$ is the distance from the folded state to the transition state; k_B the Boltzmann constant; and T the temperature in Kelvin. We obtained $X^{\ddagger}$ of 0.7 nm for breaking of the KC30 kissing complex. This value is comparable to the previous measurement (1). For the KC15, we derived $X^{\ddagger}$ of 1.15 nm. We also used a fitting algorithm by Dudko et al (3, 4). Results from the two analyses were similar.

Supplementary Figure 4. Distribution of the kissing forces of the KC30 RNA.

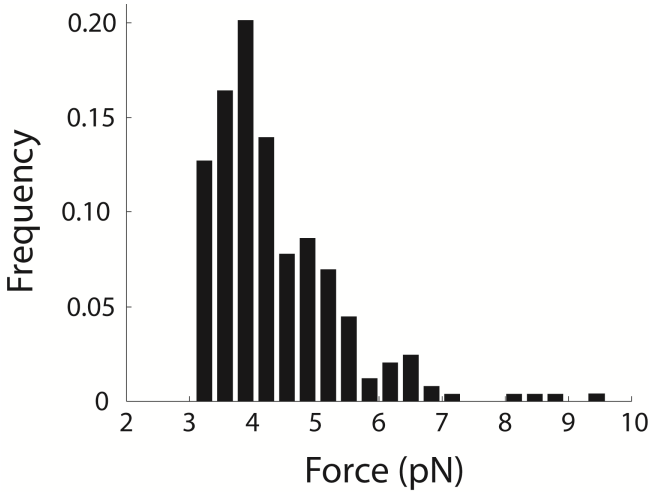

Supplementary Figure 5. End-to-end distance of a single-stranded RNA at zero force.

The end-to-end distance of a polymer, R, was computed using the worm-like-chain model (5, 6). The mean square of *R* is defined by the following equation

$$< R^2 >= 2PL[1 - \frac{P}{L}(1 - e^{-L/P})]$$

in which *P* is the persistence length, and *L* is the contour length. For single-stranded RNA, we used P = 1 nm, and *L* = 0.59 nm/nucleotide. A 30-nucleotide single strand has a mean value of *R* of 5.779 nm.

Supplementary References

1. Li, P. T. X., C. Bustamante, and I. Tinoco, Jr. 2006. Unusual Mechanical Stability of A Minimal RNA Kissing Complex. Proc. Natl. Acad. Sci. U. S. A. 103:15847-15852.
2. Evans, E., and K. Ritchie. 1997. Dynamic strength of molecular adhesion bonds. Biophys. J. 72:1541-1555.
3. Dudko, O. K., G. Hummer, and A. Szabo. 2008. Theory, analysis, and interpretation of single-molecule force spectroscopy experiments. Proc. Natl. Acad. Sci. U. S. A. 105:15755-15760.
4. Dudko, O. K., J. Mathé, A. Szabo, and G. Hummer. 2007. Extracting kinetics from single-molecule force spectroscopy: nanopore unzipping of DNA hairpins. Biophys. J. 92:4188-4195.
5. Kratky, O., and G. Porod. 1949. Röntgenuntersuchung gelöster Fadenmoleküle. Recueil des Travaux 68:1106-1122.
6. Peters, J. P., and L. J. Maher. 2010. DNA curvature and flexibility in vitro and in vivo. Q. Rev. Biophys. 43:23-63.